

UNCLASSIFIED

AD NUMBER
ADB263708
NEW LIMITATION CHANGE
TO Approved for public release, distribution unlimited
FROM Distribution authorized to U.S. Gov't. agencies only; Proprietary Info.; Sep 2000. Other requests shall be referred to U.S. Army Medical Research and Materiel Command, 504 Scott St., Fort Detrick, MD 21702-5012.
AUTHORITY
USAMRMC ltr, 26 Nov 2002

THIS PAGE IS UNCLASSIFIED

AD _____

Award Number: DAMD17-99-1-9251

TITLE: Rapid, High Resolution 3-D Ultrasound Tomography

PRINCIPAL INVESTIGATOR: Jeffrey S. Kallman, Ph.D.

CONTRACTING ORGANIZATION: Lawrence Livermore National Laboratory
Livermore, California 94550

REPORT DATE: September 2000

TYPE OF REPORT: Annual

PREPARED FOR: U.S. Army Medical Research and Materiel Command
Fort Detrick, Maryland 21702-5012

DISTRIBUTION STATEMENT: Distribution authorized to U.S. Government agencies only (proprietary information, Sep 00). Other requests for this document shall be referred to U.S. Army Medical Research and Materiel Command, 504 Scott Street, Fort Detrick, Maryland 21702-5012.

The views, opinions and/or findings contained in this report are those of the author(s) and should not be construed as an official Department of the Army position, policy or decision unless so designated by other documentation.

NOTICE

USING GOVERNMENT DRAWINGS, SPECIFICATIONS, OR OTHER DATA INCLUDED IN THIS DOCUMENT FOR ANY PURPOSE OTHER THAN GOVERNMENT PROCUREMENT DOES NOT IN ANY WAY OBLIGATE THE U.S. GOVERNMENT. THE FACT THAT THE GOVERNMENT FORMULATED OR SUPPLIED THE DRAWINGS, SPECIFICATIONS, OR OTHER DATA DOES NOT LICENSE THE HOLDER OR ANY OTHER PERSON OR CORPORATION; OR CONVEY ANY RIGHTS OR PERMISSION TO MANUFACTURE, USE, OR SELL ANY PATENTED INVENTION THAT MAY RELATE TO THEM.

LIMITED RIGHTS LEGEND

Award Number: DAMD17-99-1-9251

Organization: Lawrence Livermore National Laboratory

Those portions of the technical data contained in this report marked as limited rights data shall not, without the written permission of the above contractor, be (a) released or disclosed outside the government, (b) used by the Government for manufacture or, in the case of computer software documentation, for preparing the same or similar computer software, or (c) used by a party other than the Government, except that the Government may release or disclose technical data to persons outside the Government, or permit the use of technical data by such persons, if (i) such release, disclosure, or use is necessary for emergency repair or overhaul or (ii) is a release or disclosure of technical data (other than detailed manufacturing or process data) to, or use of such data by, a foreign government that is in the interest of the Government and is required for evaluational or informational purposes, provided in either case that such release, disclosure or use is made subject to a prohibition that the person to whom the data is released or disclosed may not further use, release or disclose such data, and the contractor or subcontractor or subcontractor asserting the restriction is notified of such release, disclosure or use. This legend, together with the indications of the portions of this data which are subject to such limitations, shall be included on any reproduction hereof which includes any part of the portions subject to such limitations.

THIS TECHNICAL REPORT HAS BEEN REVIEWED AND IS APPROVED FOR PUBLICATION.

Kath Mm 2/7/01

REPORT DOCUMENTATION PAGEForm Approved
OMB No. 074-0188

Public reporting burden for this collection of information is estimated to average 1 hour per response, including the time for reviewing instructions, searching existing data sources, gathering and maintaining the data needed, and completing and reviewing this collection of information. Send comments regarding this burden estimate or any other aspect of this collection of information, including suggestions for reducing this burden to Washington Headquarters Services, Directorate for Information Operations and Reports, 1215 Jefferson Davis Highway, Suite 1204, Arlington, VA 22202-4302, and to the Office of Management and Budget, Paperwork Reduction Project (0704-0188), Washington, DC 20503.

1. AGENCY USE ONLY (Leave blank)		2. REPORT DATE September 2000	3. REPORT TYPE AND DATES COVERED Annual (1 Sep 99 - 31 Aug 00)	
4. TITLE AND SUBTITLE Rapid, High Resolution 3-D Ultrasound Tomography			5. FUNDING NUMBERS DAMD17-99-1-9251	
6. AUTHOR(S) Jeffrey S. Kallman, Ph.D.				
7. PERFORMING ORGANIZATION NAME(S) AND ADDRESS(ES) Lawrence Livermore National Laboratory P. O. Box 808, L-154 Livermore, California 94550 E-MAIL: kallman1@llnl.gov			8. PERFORMING ORGANIZATION REPORT NUMBER	
9. SPONSORING / MONITORING AGENCY NAME(S) AND ADDRESS(ES) U.S. Army Medical Research and Materiel Command Fort Detrick, Maryland 21702-5012			10. SPONSORING / MONITORING AGENCY REPORT NUMBER	
11. SUPPLEMENTARY NOTES				
12a. DISTRIBUTION / AVAILABILITY STATEMENT Distribution authorized to U.S. Government agencies only (proprietary information, Sep 00). Other requests for this document shall be referred to U.S. Army Medical Research and Materiel Command, 504 Scott Street, Fort Detrick, Maryland 21702-5012.			12b. DISTRIBUTION CODE	
13. ABSTRACT (Maximum 200 Words) Ultrasonic transmission tomography holds out the hope of being a discriminating tool for breast cancer screening that is safe, comfortable, and inexpensive. From its inception, however, this imaging modality has been plagued by the problem of how to quickly and inexpensively obtain the data necessary for the tomographic reconstruction. The specific aim of this research is to determine how best to adapt a new microfabricated ultrasonic sensor (currently under development for defense applications) into a breast cancer screening tool. The sensor converts an acoustic wavefront into a modulated optical signal over an entire imaging plane. Using this device, it should be possible to obtain the data necessary for 3D imaging of a breast in a short time, without ionizing radiation, and without the need for compression of the breast. The research for the first year has focused on refinement of the sensor design and development of reconstruction algorithms. In this first year, we have automated the acquisition of the data, increased the speed of data acquisition by a factor of 100, increased the robustness of the sensor, incorporated a rotation stage in our test tank, and acquired and imaged diffraction tomographic data from a phantom.				
14. SUBJECT TERMS Breast Cancer, ultrasound, transmission ultrasound, opto-acoustic imaging, early detection.			15. NUMBER OF PAGES 18	
			16. PRICE CODE	
17. SECURITY CLASSIFICATION OF REPORT Unclassified	18. SECURITY CLASSIFICATION OF THIS PAGE Unclassified	19. SECURITY CLASSIFICATION OF ABSTRACT Unclassified	20. LIMITATION OF ABSTRACT Unlimited	

NSN 7540-01-280-5500

Standard Form 298 (Rev. 2-89)
Prescribed by ANSI Std. Z39-18
298-102

20010302 072

Table of Contents

Cover.....	
SF298.....	2
Table of Contents.....	3
Introduction.....	4
Body.....	5-14
Key Research Accomplishments.....	15
Reportable Outcomes.....	15
Conclusions.....	16
References.....	17

INTRODUCTION:

Ultrasonic transmission tomography holds out the hope of being a discriminating tool for breast cancer screening that is safe, comfortable, and inexpensive. From its inception, however, this imaging modality has been plagued by the problem of how to quickly and inexpensively obtain the data necessary for the tomographic reconstruction. The specific aim of this research is to determine how best to adapt a new microfabricated ultrasonic sensor (currently under development for defense applications) into a breast cancer screening tool. The sensor converts an acoustic wavefront into a modulated optical signal over an entire imaging plane. Using this device, it should be possible to obtain the data necessary for 3D imaging of a breast in a short time, without ionizing radiation, and without the need for compression of the breast. The research for the first year has focused on refinement of the sensor design and development of reconstruction algorithms.

Annual Report Body:

In this report we detail the first year of development and design of our optically parallel ultrasound sensor (OPUS). The tasks that were addressed in this first year were: sensor refinement, reconstruction algorithm development, and sensor calibration. Additionally, we began performing next year's phantom tank studies.

BACKGROUND:

Scientific Basis:

The basic physical principle we are using to do ultrasonic sensing is frustrated total internal reflection (a consequence of optical refraction)^{1,2}. Refraction occurs when a wave crosses an interface between media in which the speeds of light are different (i.e. of different refractive indices) [Snell's Law]. If light moves from a slow medium to a fast one, there is a critical angle, $\theta_c = \sin^{-1}(n_1/n_2)$ (where n_2 is the index of refraction of the slow medium and n_1 is the index in the fast medium), beyond which the light is totally reflected. This simple picture ignores the evanescent wave, which extends outside the high index medium, falls off exponentially in amplitude to almost zero within one wavelength beyond the interface, and does not propagate. Frustrated total internal reflection occurs when another slow medium intercepts the evanescent wave. Some light tunnels through the gap and propagates into that medium. The amount of light that tunnels is related to the materials involved, the polarization, and the gap width (see Figures 1 and 2).

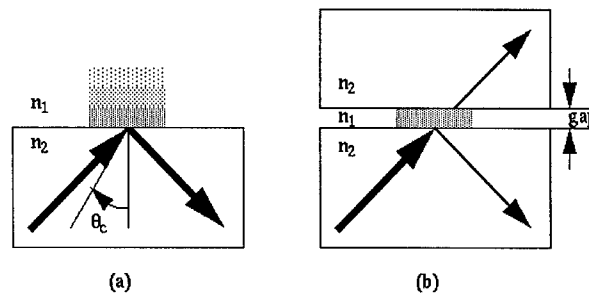


Figure 1. (a) Total internal reflection (TIR) occurring at the interface between an optically slow medium (n_2) and a fast medium (n_1). The evanescent wave extends into the fast medium. (b) Frustrated total internal reflection occurs when another slow medium intercepts the evanescent wave.

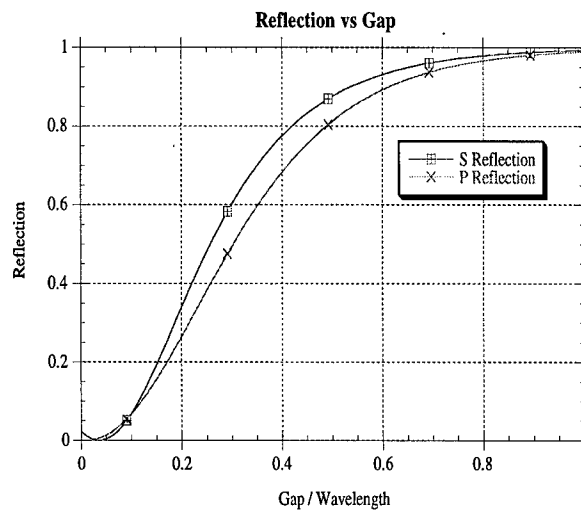


Figure 2. Reflection vs. gap size at the interface between slow and fast media.

Our new sensor uses frustrated total internal reflection to make an incident ultrasonic wave modulate a pulsed beam of light, which is then acquired by a camera and computer. A sequence of images, each taken with the optical pulse at a different source acoustic phase, enables us to reconstruct the ultrasonic phase and amplitude over an entire 2-D surface.

Optics:

We can exploit frustrated total internal reflection by building an array of acoustic pixels. Each acoustic pixel is composed of a thin (0.1 micron) silicon nitride membrane suspended on short (0.2 micron) gold walls over an optical substrate. The gap between the membrane and the optical substrate is filled with air (figure 3). The membrane is exposed to the ultrasonic couplant. When an ultrasonic pressure wave travels through the couplant and impinges on the acoustic pixel, the membrane deflects, causing a change in the amount of light reflected from the total internal reflection surface of the acoustic pixel. An array of acoustic pixels can be used to modulate a beam of light.

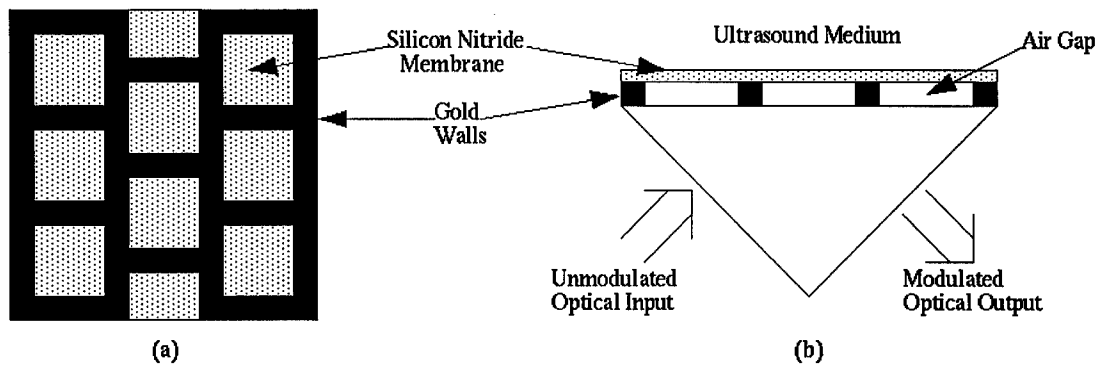


Figure 3. (a) Top view of an array of acoustic pixels. (b) Side view showing acoustic pixels mounted on optical substrate

Just as a strobe light can be used to watch the vibration of a drumhead, we are using a strobed optical source to watch the relative phases and amplitudes of tens of thousands of acoustic pixels, all at once. Given a sequence of images and calibration data, we can extract the relative phase and amplitude of the vibration, and thus extract the relative pressure phase and amplitude at each acoustic pixel. To obtain this information we illuminate the sensor with ten sequences of optical pulses, each sequence timed to act as a strobe light at a specific acoustic phase (figure 4).

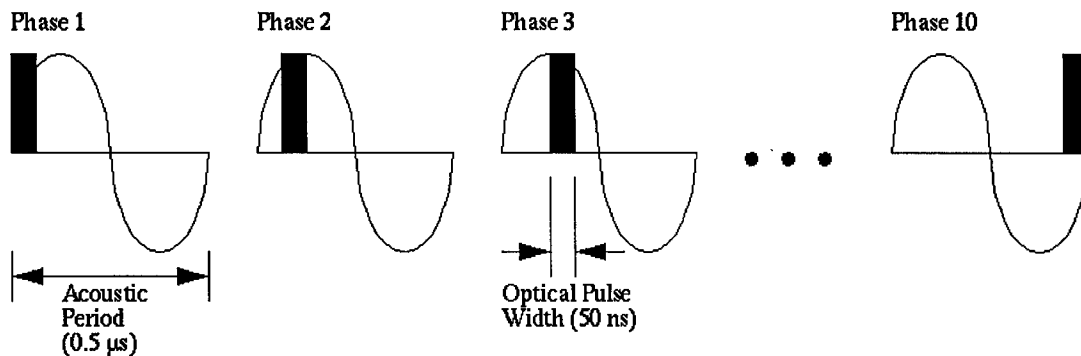


Figure 4. Ten images are taken, each with the optical pulse at a different position in the acoustic period.

We extract the phase and amplitude at each pixel by fitting the intensity at that pixel through the sequence to the form $I = B + A \sin(2\pi i / 10 + C)$ where I is the intensity, B is the background, A is the amplitude of the sinusoidal variation, i is the index of the image in the sequence, and C is the phase of the variation.

The optical train of this device is as follows: we illuminate the sensor using an LED, the light from which is homogenized, polarized, and collimated. We acquire the reflection using either a CCD still camera or a video camera.

Acoustics:

The imaging technique we are interested in is transmission ultrasound. In this modality, an acoustic source sends out a pressure wave through a couplant, such as water, oil, or medical ultrasound gel, to the object of interest. The pressure waves are transmitted through the object, being modified in amplitude and phase along the way. The pressure wave emerges from the object of interest and travels, via the couplant, to our acoustic sensor.

Our sensor works because the pressure wave flexes a membrane, causing it to vibrate with a phase and amplitude that are functions of that wave. In designing our sensor, we needed to have a membrane with a frequency response high enough to vibrate at the frequencies of interest to us (approximately 2 MHz).

Design Parameters:

There are many material and operational parameters that must be chosen correctly in order to make a working OPUS. Among these are the membrane and wall materials, membrane thickness, wall height, acoustic pixel size, ultrasound operating frequency, optical source characteristics, optical pulse characteristics, and camera characteristics.

Some of these parameters were simple to choose, such as the material for the membrane. The fabrication processes available to us restricted our choice of membrane materials to silicon and silicon nitride. As we wanted to do this work with visible light, we chose to use a silicon nitride membrane.

Other parameters were more difficult to choose, as there was significant interaction between them. For instance, the membrane thickness and the acoustic pixel size interact with each other to effect the sensitivity and frequency response of the sensor. Thus, we relied on modeling to narrow the ranges of these parameters.

Fabrication:

The membrane and its supports are fabricated as depicted in Figure 5.

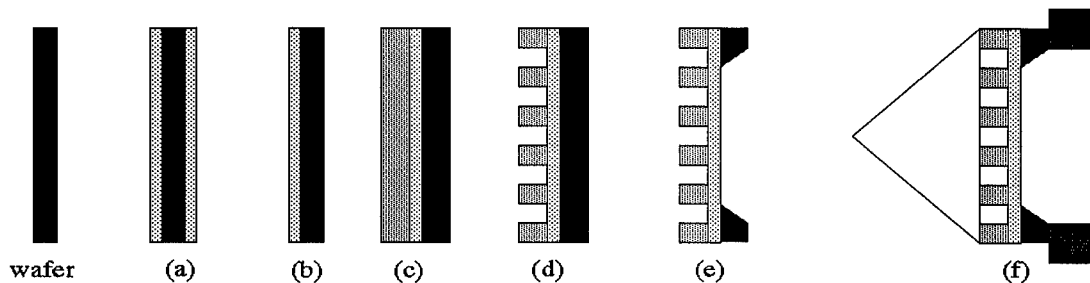


Figure 5. (a) The silicon wafer has nitride deposited on both sides. (b) The nitride is etched away on one side. (c) A layer of gold is deposited on the nitride. (d) The gold is etched to leave support walls. (e) The silicon is etched from the back, leaving a frame that supports the whole system. (f) The membrane and walls are bonded to the optical substrate, and then mounted to the support plate.

Sensor Parameters:

As a result of proof-of-principle experiments, we had the information necessary for the design and fabrication of the first generation sensor. The acoustic pixel size is 70 microns square, with a 0.1 micron thick membrane, mounted on walls 0.2 microns high. The active aperture is 7 mm square. The sensor is currently being operated at a frequency of 2MHz, at acoustic powers of 20-200 mW/cm².

Sensor Noise Characteristics:

The CCD camera we are using is an Apogee Instruments AP1. The images it provides are 760 x 510 pixels, each of which is 16 bits deep. We expose the CCD for one second (two million pulses). We are using a HP 214B pulse generator to send 50 nanosecond 2.8 volt pulses to a red LED.

To determine the purely optical noise characteristics of our data, we collected a set of 40 images with no acoustic excitation. The noise is approximately Gaussian with standard deviations extending from 24 to 60 counts. In taking data, with the acoustic and optical parameters as above, we collect 90 sequences of images and average, reducing the noise by a factor of 9. The expected sinusoidal variation in our data had amplitudes ranging from 30 to 100 counts.

Data Acquisition System:

The data acquisition system consists of an OPUSensor, a tank with an acoustic source and object of interest, and the optics. The system is illustrated in schematic form in figure 6. A Telulex SG-100A arbitrary waveform generator (AWG) provides both a 2 MHz CW signal and an optical pulse synchronization signal. This waveform generator has the ability to generate an arbitrary waveform (which we used to produce a 2 MHz sinewave to send to the amplifier) and an arbitrary sync pulse (which we used to drive the optical pulse generator) simultaneously, under computer control. The 2 MHz sinusoid is amplified and fed through the power meter to the acoustic source in the water tank. The sync signal goes to the pulse generator, which in turn excites the optical source as a strobe light. The pulse generator output and the oscillator output are both fed to an oscilloscope to allow the user to place the optical pulse at any point in the acoustic phase, although this is usually under computer control. The optical pulses are homogenized, polarized, collimated, and fed through the prism to the sensing surface, and the reflected light is captured by the camera and saved in the computer. The user has control over the oscillator frequency, the amplifier gain, the camera exposure time, the optical pulse width, amplitude, and placement in the acoustic phase, as well as the depth of the water in the tank.

During a typical experimental run the water tank was filled to the desired depth, and the acoustic power level, camera exposure time, optical pulse width, and optical pulse amplitude were set.

The object of interest was positioned between the acoustic source and the sensor. Sequences of ten images were acquired, each with the optical pulse occurring at a different acoustic phase. Both object data and calibration data (without the target) were acquired.

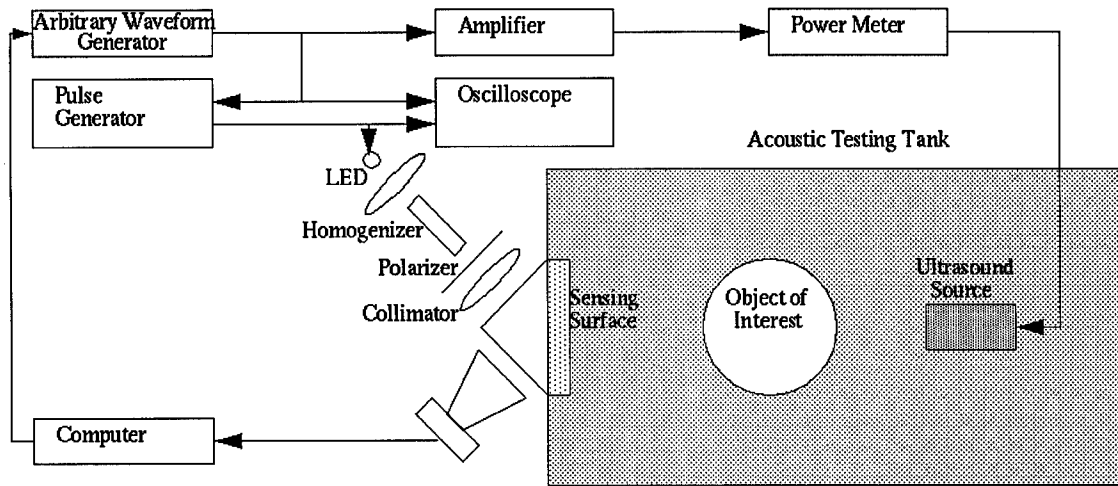


Figure 6. Schematic view of the data acquisition system. The arbitrary waveform generator output is sent to the amplifier (to provide the acoustic signal to the transducer) and the pulse generator (to provide the optical signal). The optical pulse is homogenized, polarized, collimated and sent to the sensing surface. Upon reflection it is acquired by the computer controlled camera. The object of interest is optional.

CURRENT YEAR TASKS:

Task 1: Sensor Refinement.

The refinement of the sensors is to be a continuous process over the two years of the grant. Sensor refinement entails optimizing sensitivity, improving manufacturing techniques, and increasing the speed of data acquisition.

We continue to experiment with modifications to the sensor membrane to improve the sensitivity. We have found that because the resonances of the acoustic pixels are so broad, there is little to be gained by adjusting their area for acoustic optimality. Instead we have increased the acoustic pixel size slightly so as to increase the area for optical illumination and improve our optical signal to noise ratio.

We have made four design changes to the sensor:

- We changed the way that the sensor and prism are assembled. Previously, sensors were assembled by taking a porthole, laying the sensor on top, then gluing a prism over the top. This turned out to be a suboptimal assembly technique, often leading to leaks around the membrane frame and destroyed sensors. Now, we glue the membrane frame to the plate and then press the prism against the membrane, supporting the prism from the rear with a frame attached to the plate. This insures that the membrane frame will not leak, and it allows easier pre-installation testing of the membranes for water-tightness.
- We increased the robustness of the membrane. Originally, our membranes were fabricated under high tension (500MPa). By altering the fabrication parameters, lower tension (100MPa) membranes were produced. Prior to this change, membranes would rupture at the

slightest provocation. With the lower tension membranes, the membranes last indefinitely (no failures since the change).

- The sensor membrane size was adjusted from 1cm on a side to 0.7 cm on a side. Although this reduced the aperture size, it improved the sensor fabrication yield and robustness.
- We began the process of scaling up the sensor aperture by using paned windows of the .7 x .7 cm membranes. We have designed and fabricated membranes consisting of a 5 x 3 paned array, with at least a 90% active area. This is pending assembly into a new sensor.

By changing from our Apogee digital camera to a video camera, we have reduced acquisition times by a factor of approximately 100. The Apogee camera required 1 second to acquire a frame of data and 8 seconds to offload it into the computer. We are able to acquire video images at a rate of 10 frames per second. This has significantly changed the way we acquire data. Previously, we set the optical pulse at a specific acoustic phase for each image acquired. This added additional time to each frame acquired, but spread long-term drifts in the data acquisition system parameters over all phases. This was important because it could take 3 hours to collect a sequence of data. Now we can set the optical pulse in the acoustic phase and acquire all the frames we wish to average in less than 10 seconds. Unfortunately, the borrowed video camera is noisier than the Apogee camera. However, by acquiring more frames we can reduce the noise.

In switching to a video camera we have qualitatively changed the way the sensor can be used. We have found that at video speeds the eye's filtering ability enables one to see changes in the pressure wavefronts impinging on the sensor in real time. By changing the timing of the optical pulse, one can infer the shape of the wavefront.

Task 2: Reconstruction Algorithm Development.

As a crucial step in verification of any reconstruction algorithm, a simulator had to be developed that could model both the propagation of sound through a phantom and reconstruction of images using the data. We built the simulator, based on the BEEMER scalar paraxial wave propagation code. This allowed us to import simulated phantoms, model the propagation of sound through them, and experiment with reconstruction algorithms. We used a Rytov-approximation based, filtered backpropagation algorithm³ to do the 2D reconstruction experiments.

The two most commonly used simplifications in linear diffraction tomography are the Born and Rytov approximations. The Born approximation assumes that there are no large differences in the index of refraction anywhere in the problem space^{4,5}. The Rytov approximation assumes that there are no large gradients in the index of refraction⁶. Both assume that there is no multiple scattering. Devaney first published the filtered backpropagation algorithm in 1982³. Filtered backpropagation uses a more general form of the Fourier projection-slice theorem, and reduces to filtered backprojection in the zero wavelength limit. Whereas the Fourier transform of a zero wavelength projection in real space equals a radial slice of Fourier space perpendicular to the angle of the projection, the Fourier transform of a finite wavelength projection is equal to a semicircle in Fourier space which grazes the origin at an angle perpendicular to the angle of the projection (see figure 7). In the zero wavelength limit, filtered backprojection is a fast and simple way to reconstruct images from projections⁷. In the case of finite wavelength, filtered backpropagation is an attractive reconstruction method. With filtered backprojection, the projection is filtered and then distributed into the reconstruction space to generate an image. Filtered backpropagation requires that the filtered projection be propagated across the reconstruction space. Propagation is a more computationally intense operation than simple projection.

Based on the experiments we performed with the simulator, we built a stand-alone 2D reconstruction code which used a simple implementation of the Devaney Rytov filtered backpropagation

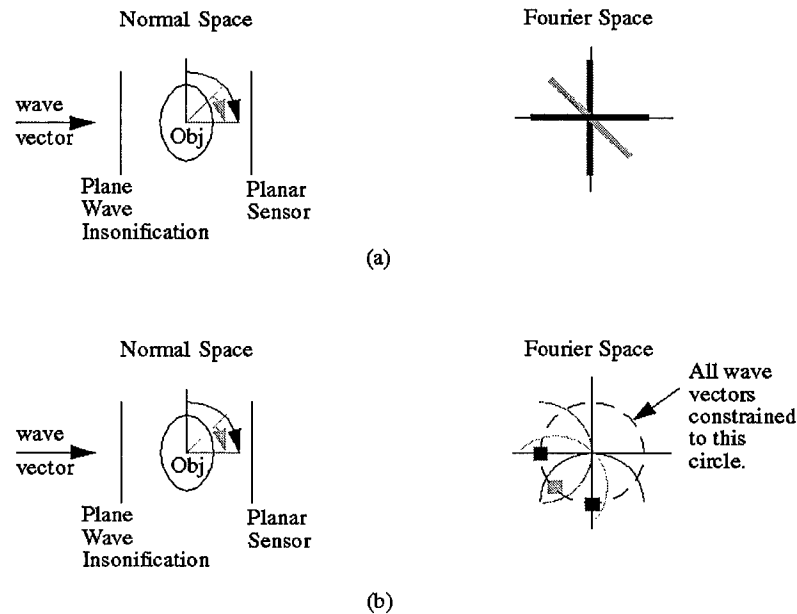


Figure 7. The difference between zero and finite wavelength projections: a) zero wavelength limit, Fourier transforms of projections become radial lines, b) finite wavelengths, Fourier transforms of projections become semicircles.

Task 3: Sensor Calibration.

Because we have developed experimental protocols that include normalizing the subject data to calibration images, optical calibration is unnecessary. Thus, even though the illumination is not uniform over the whole sensor, the calibration images normalize out the nonuniformities.

We have determined that the acoustic response of the sensor is linear. We acquired data using 10 different input voltage levels (0.0V peak to peak to 9.0V peak to peak to the amplifier) (see figure 6). We collected sequences of data for each of these levels and extracted from them the amplitudes at each acoustic pixel. The amplitude vs. power level at each pixel is linear, with correlation coefficient of 0.984. The highly linear nature of the data indicates that the deflections of the membrane are very small because (as can be seen in figure 2) a large deflection would have excited the sensor into the nonlinear portion of the optical response curve.

By measuring the power input to the source transducer, we have determined the minimum pressure required to optically observe deflection of the membrane. The membrane can detect pressure changes of 7kPa (actually, considering the efficiency and location of the source transducer, it is likely seeing at least a factor of 10 smaller pressure).

Task 4: Phantom Tank Studies.

Diffraction Tomography Experiments:

For a test of diffraction tomography using the sensor we built a phantom with a constant 2D cross section. The phantom consisted of three pieces of 0.5mm diameter fishing line placed at 120 degree separations around a 1.5 mm radius circle (see figure 8). These materials and configuration were selected because the plastic has an acoustic index not too different from the liquid medium (a situation that mimics the variability in acoustic index in the breast), and the

sizes are comparable to what we plan to image with the system. We used water as our acoustic medium; therefore, an acoustic frequency of 2 MHz had a wavelength of 0.74 mm. Using our simulator (a modification of the BEEMER modeling code⁸) we determined that it would be possible to do a diffraction tomographic reconstruction with 18 projections.

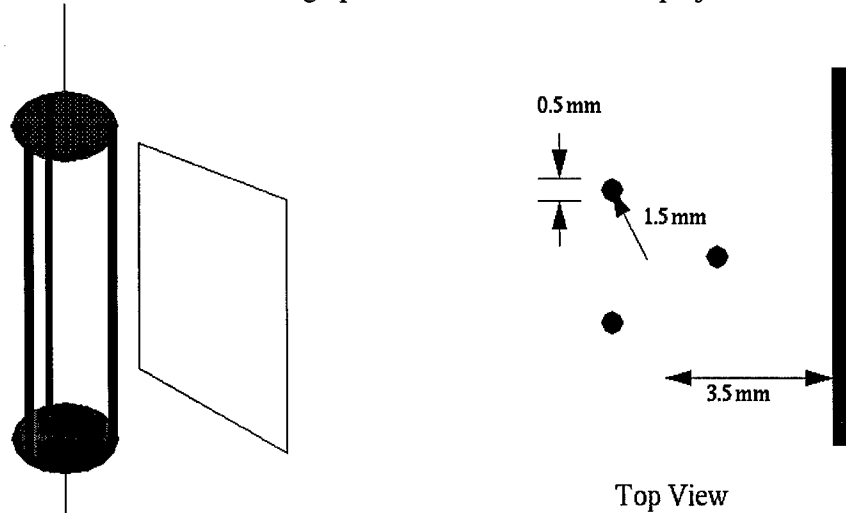


Figure 8. The relationship and dimensions of the phantom and the sensor.

We utilized a constant cross-section phantom so that 2D reconstruction (rather than 3D) could be performed. The full 3D reconstruction algorithms are still under development.

Equipment Modifications:

We mounted a rotation stage above the tank and suspended the phantom 3.5 mm in front of the sensor. The rotation stage was manually controlled. We mounted the source transducer far enough away (10 cm) to illuminate the phantom with a planar 2MHz ultrasound wave.

Data Acquisition:

The data necessary for reconstruction of the phantom are a set of 18 projections, where each projection consists of the relative acoustic phase and amplitude over the entire sensor surface. The acoustic period was divided into ten discrete phases, as sufficient to extract the sinusoidal parameters at each acoustic pixel. A set of 10 images is a sequence from which phase and amplitude can be extracted. We took 90 sequences that were then summed, to increase the signal to noise ratio.

The data for each projection (18 projections overall) were acquired under computer control. The data consisted of 90 sequences of 10 images (one image with the optical pulse at each of 10 acoustic phases). To acquire each image, the sinusoidal waveform was downloaded into the arbitrary waveform generator with the sync pulse at the appropriate acoustic phase, the camera shutter was opened for 1 second, then the data was downloaded to the computer. The image was summed into a composite image for the appropriate phase. Upon completion of the acquisition of the 90 sequences, the final summed images were saved to disk. After each projection was acquired, the phantom was rotated 20 degrees, and acquisition was repeated.

After the projection data were acquired, we obtained calibration data by removing the phantom and averaging 90 sequences of 10 phase images.

This page contains unpublished data. Limited distribution only.

Data Reduction:

After data collection we had 18 projection sequences and one calibration sequence, each consisting of 10 summed images. For each pixel in every sequence, the intensity was fit to a sinusoid with phase plus a background. Since the illumination over the optical field was not uniform (intentionally, to minimize costs), the sinusoidal amplitude was normalized by the background intensity. For every pixel in each sequence we recorded the amplitude ratio and the phase. To extract relative pressure amplitude, we normalize the image of the projection ratios by the image of the calibration ratios, on a pixel by pixel basis. This yielded 18 images of relative pressure amplitude (see figure 9). By subtracting the calibration phase from the target phases, we obtained 18 images of relative phase.

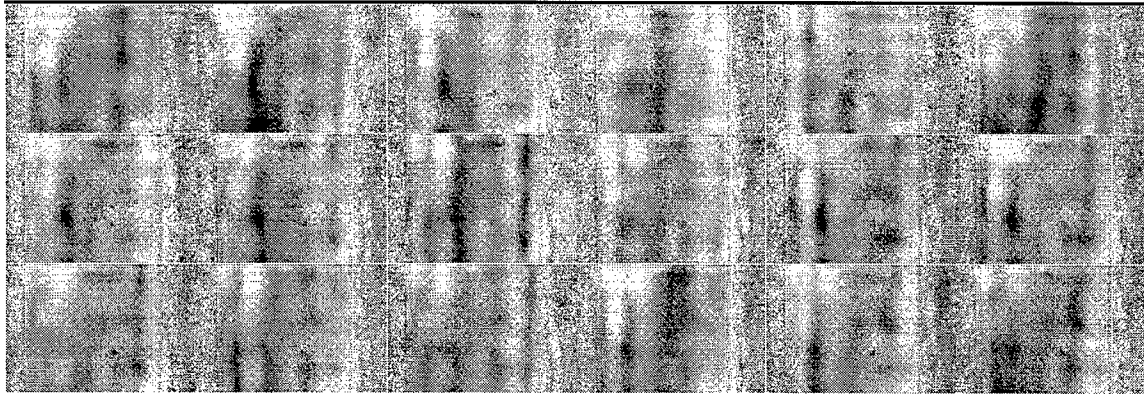


Figure 9. The 18 images of relative pressure amplitude obtained by the OPUS system from the 3-monofilament phantom.

Image Reconstruction:

Using a simple implementation of the Devaney Rytov filtered backpropagation (see task 2 above), we were able to obtain images of both the distributions of sound speed and absorption (see figure 10).

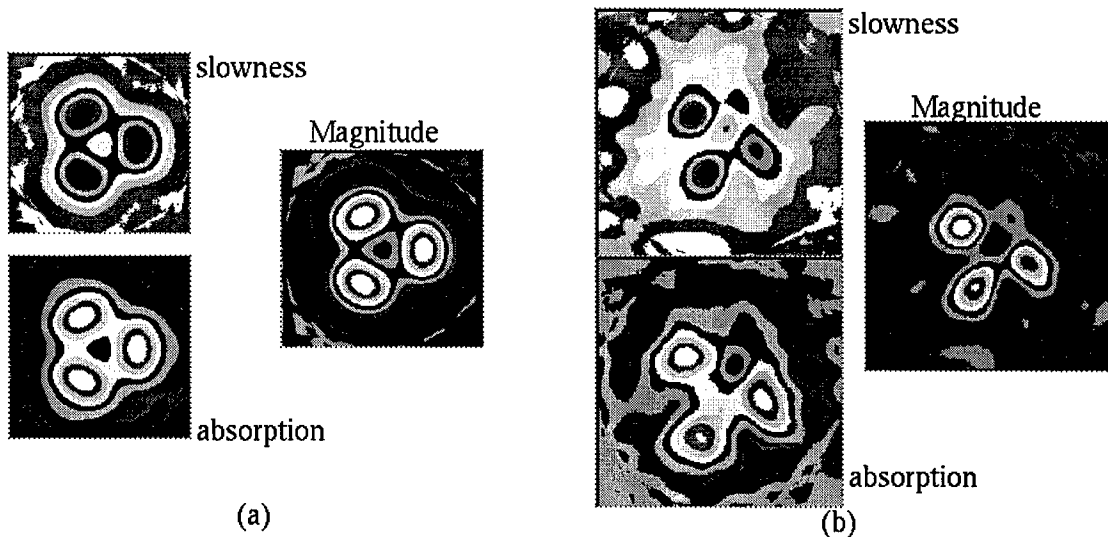


Figure 10. a) Reconstruction of a simulation of the 3-monofilament phantom using Devaney-Rytov filtered backpropagation. b) Reconstruction from the data in figure 9.

This page contains unpublished data. Limited distribution only.

SUMMARY:

We have developed a new type of ultrasound sensor that makes it possible to sense the pressure field over a plane. The sensor uses the phenomenon of frustrated total internal reflection to modulate the reflection of an optical beam depending on the deflection of a 0.1 micron thick silicon nitride membrane that covers an acoustic pixel. Our acoustic pixels are defined by gold walls 0.2 microns tall and enclosing a square air space approximately 70 microns on a side. We have used an array of 10,000 acoustic pixels to acquire data yielding diffraction tomographic images of a 3-monofilament phantom.

We have improved the sensor speed and robustness. We have implemented a 2D reconstruction algorithm. We have developed acquisition protocols that obviate the need for optical calibration, and have performed an acoustical calibration. In addition, we began next year's tasks by building a phantom tank with rotation stage and imaging a phantom.

FUTURE WORK:**Speed**

We are in the process of making data acquisition much faster. The use of a borrowed video camera has sped the acquisition of data by a factor of approximately 100. We plan to purchase a high quality video camera next fiscal year. The higher sensitivity of the new camera will reduce the number of images that have to be summed to maintain the same signal to noise ratio. Thus, it will make data acquisition even faster.

Scaling Challenges

In order to make this sensor useful for medical applications, we are scaling up the sensing aperture for the OPUS. It would be difficult to construct large free standing membranes. We are circumventing that difficulty by building mosaics of 0.7 cm windows.

Data Reconstruction

In addition to diffraction tomography, we are looking into the use of adjoint methods for the reconstruction of diffraction data^{9,10}. Because we now anticipate the development of reconstruction algorithms to be more time consuming than originally thought, we are pleased to be slightly ahead of schedule for Task 4. Thus, we should continue on schedule through the second fiscal year.

ACKNOWLEDGEMENTS:

This work was performed under the auspices of the U.S. Department of Energy by Lawrence Livermore National Laboratory under contract W-7405-Eng-48.

This work was sponsored by the Department of the Army (Breast Cancer Research Program) under contract DAMD 17-99-1-9251. The U.S. Army Medical Research Acquisition Activity, 820 Chandler Street, Fort Detrick, MD 21702-5014 is the awarding and administering acquisition office. The content of this report does not necessarily reflect the position or the policy of the Government, and no official endorsement should be inferred.

This page contains unpublished data. Limited distribution only.

KEY RESEARCH ACCOMPLISHMENTS:

Sensor Refinement

- We changed the fabrication process to generate low-tension membranes in 0.7 cm square-frames. These proved far more durable than high-tension membranes in 1.0 cm square-frames.
- We determined that an acoustic pixel size of 70 microns is appropriate for excitation frequencies of up to 2 MHz.
- We incorporated a video-rate camera for data acquisition. It not only increased the speed of acquisition by a factor of 100 but also made the system more like a fluoroscope in that one could watch changes in the acoustic pressure waveform in real-time.

Reconstruction Algorithm Development

- We discovered that our sensor can collect data with a high enough signal to noise ratio that they can be reconstructed into an image.
- We determined that linear approximations were sufficient for reconstructing our phantom data.

Sensor Calibration:

- We implemented data acquisition protocols such that no prior optical calibration is necessary because optical calibration data are acquired as a part of normal data acquisition.
- We determined that the sensor is linear in its response to acoustic excitation.
- We demonstrated that the sensor can detect pressure amplitudes below 7 kPa.

Phantom Tank Studies

- We modified the test tank to be used for phantom studies.
- We acquired data from a simple phantom.
- We reconstructed images using linear diffraction tomography.

REPORTABLE OUTCOMES:

- We have a manuscript in preparation for submission to Journal of the Acoustical Society of America.

CONCLUSIONS:

We have developed a new type of ultrasound sensor that makes it possible to sense the pressure field over a plane. The sensor uses the phenomenon of frustrated total internal reflection to modulate the reflection of an optical beam depending on the deflection of a 0.1 micron thick silicon nitride membrane that covers an acoustic pixel. Our acoustic pixels are defined by gold walls 0.2 microns tall and enclosing a square air space approximately 70 microns on a side. We have used an array of 10,000 acoustic pixels to acquire data yielding diffraction tomographic images of a 3-monofilament phantom.

We have improved the sensor speed and robustness. We have implemented a 2D reconstruction algorithm. We have developed acquisition protocols that obviate the need for optical calibration, and have performed an acoustical calibration. In addition, we began next year's tasks by building a phantom tank with rotation stage and imaging a phantom.

The development of this technology is important for the early detection of breast cancer. It offers a potential way of implementing volumetric imaging of the breast without the ionizing radiation and discomfort of x-ray mammography or the cost of MRI. To fulfill this promise, we must scale up the sensor and develop further reconstruction algorithms.

REFERENCES:

1. J. Strong, *Concepts of Classical Optics*, W. H. Freeman and Company, 1958.
2. P. Yeh, *Optical Waves in Layered Media*, John Wiley and Sons, New York, 1988.
3. A. J. Devaney, "A filtered backpropagation algorithm for diffraction tomography," *Ultrasonic Imaging*, **4**, pp. 336-350, 1982.
4. E. Wolf, "Three-Dimensional Structure Determination of Semi-Transparent Objects From Holographic Data," *Optics Communications*, **1**, pp. 153-156, 1969.
5. R. Dandliker and K. Weiss, "Reconstruction of the Three-Dimensional Refractive Index From Scattered Waves," *Optics Communications*, **1**, pp. 323-328, 1970.
6. A. J. Devaney, "Inverse-scattering theory within the Rytov approximation," *Optics Letters*, **6**, pp. 374-376, 1981.
7. A. Makovski, *Medical Imaging Systems*, Prentice-Hall, Inc., pp. 125-126, 1983.
8. R. J. Hawkins, J. S. Kallman, R. W. Ziolkowski, "Computational Integrated Photonics," *Engineering Research Development and Technology*, R. T. Langland, C. Minichino, UCRL 53868-92, pp 1.7-1.11, Lawrence Livermore National Laboratory, Livermore, 1993.
9. O. Dorn, H. Bertete-Aguirre, J. G. Berryman, G. C. Papanicolaou, "A nonlinear inversion method for 3D electromagnetic imaging using adjoint fields," *Inverse Problems* **15**, pp. 1523-1558, 1999.
10. F. Natterer, F. Wubbeling, "A propagation-backpropagation method for ultrasound tomography," *Inverse Problems*, **11**, pp. 1225-1232, 1995.



DEPARTMENT OF THE ARMY
US ARMY MEDICAL RESEARCH AND MATERIEL COMMAND
504 SCOTT STREET
FORT DETRICK, MARYLAND 21702-5017

REPLY TO
ATTENTION OF:

MCMR-RMI-S (70-1y)

26 Nov 02

MEMORANDUM FOR Administrator, Defense Technical Information
Center (DTIC-OCA), 8725 John J. Kingman Road, Fort Belvoir,
VA 22060-6218

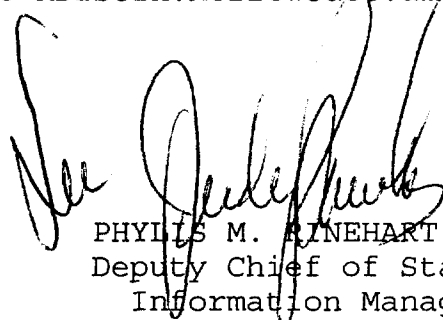
SUBJECT: Request Change in Distribution Statement

1. The U.S. Army Medical Research and Materiel Command has reexamined the need for the limitation assigned to technical reports written for this Command. Request the limited distribution statement for the enclosed accession numbers be changed to "Approved for public release; distribution unlimited." These reports should be released to the National Technical Information Service.

2. Point of contact for this request is Ms. Kristin Morrow at DSN 343-7327 or by e-mail at Kristin.Morrow@det.amedd.army.mil.

FOR THE COMMANDER:

Encl



PHYLLIS M. RINEHART
Deputy Chief of Staff for
Information Management

ADB263708
ADB257291
ADB262612
ADB266082
ADB282187
ADB263424
ADB267958
ADB282194
ADB261109
ADB274630
ADB244697
ADB282244
ADB265964
ADB248605
ADB278762
ADB264450
ADB279621
ADB261475
ADB279568
ADB262568
ADB266387
ADB279633
ADB266646
ADB258871
ADB266038
ADB258945
ADB278624